



EFFECTS OF CONFINED CONCRETE MODELS ON SIMULATING RC COLUMNS UNDER LOW-CYCLIC LOADING

Zongming HUANG¹ Wenfeng ZHOU² Tao CHEN¹ Juan CHEN¹

SUMMARY

Material models are the base of computer simulation analysis of structure. Many confined concrete models have been put forward until now; however, there are few comparative studies on effect of confined concrete models on structural member analysis. In this paper, four models are selected as the representatives and applied to nonlinear dynamic analysis program for space frames which is based on the beam-column element using the finite element flexibility method and the fiber model. Park's test on columns that are combined axial and bending under cyclic loading are taken as the calibrations, comparisons to material and structural member level are drawn and the analytical results of various models are discussed. From this study it is concluded that despite the significant difference in the stress-strain curve of each confinement model the difference in structural member analysis reduces obviously but still remarkable. The simulation using the Mander model shows better agreement with the experimental results.

INTRODUCTION

The accuracy of nonlinear analysis of RC structure depends strongly on material models. Various analytical models available in the literature for confined concrete are mostly limited to material level and comparative study on applicability of the different concrete model to RC member analysis are rarely made; however, engineer community would pay more attention to the accuracy of the model in simulation at structural or member level. An ideal confined concrete model should be the following: 1. good precision in simulation at member or structural level; 2. to reflect the dominant aspects of confinement, fewer parameters, and explicit in physics.

In this paper, four models are selected as the representatives and applied to nonlinear dynamic analysis program for space frames which is based on the beam-column element using the finite element flexibility method and the fiber model. On the basis of experimental results by Park [2], simulation and comparison are made on combined axial and bending columns under cyclic loading at material level. The effect of different hysteretic rules and skeleton curves on simulation results are investigated at material and member level respectively.

¹.College of Civil Engineering, Chongqing University, Chongqing, China.

².Quality-monitoring Station in Guangzhou, Guangzhou, China.

This work was sponsored by National Natural Science Foundation of China under Grant No.59978055

RIENFORCED CONCRETE COLUMN SPECIMEN BY PARK

In Reference 2, the effect of some factors such as different tie configuration, ratio of axial compress force to strength, volumetric ratio of transverse reinforcement and tie yield strength and concrete strength, etc had been taken into account on combined axial and bending columns under cyclic loading. The ratios of longitudinal reinforcement of four members are all 0.0179 and their yield strengths are 375Mpa. Fig.3 shows the scheme of the experiment and other more details can be referred to Reference 2.

Tab. 1 Test data shown in Reference 2

specimen	f_c (Mpa)	axial load (KN)	ratio of axial compress force to strength	section type	Volumetric ratio of transverse reinforcement	f_{yh} (MPa)	tie spacing (mm)
1	23.1	1815	0.260	A	0.015	297	80
2	41.4	2680	0.214	A	0.023	316	75
3	21.4	2719	0.420	B	0.020	297	75
4	23.5	4265	0.600	B	0.035	294	72

FIBER-MODEL BASED BESM-COLUMN ELEMENT

The experimental results of column specimens by Park were studied by applying a nonlinear analytical method to a RC section, i.e., fiber model. As is well known, the RC section would be divided into many fibers paralleled to the longitudinal axis, adopting Bernoulli-Euler's assumption, the section's moment curvature relationship was set up based on the uniaxial stress-strain relationship of the concrete and the longitudinal bar. The influence of shear and bond slip between the concrete and steel was neglected. In the concrete model, the difference in the compressive strength and descending branch between the core concrete and the cover concrete were considered. The beam-column element is cast in the framework of the finite element flexibility based beam theory by Spacone et al [9]. Finally, the Menegotto and Pinto law modified by Filippou et al [10] to include isotropic strain hardening is used for the reinforcing steel.

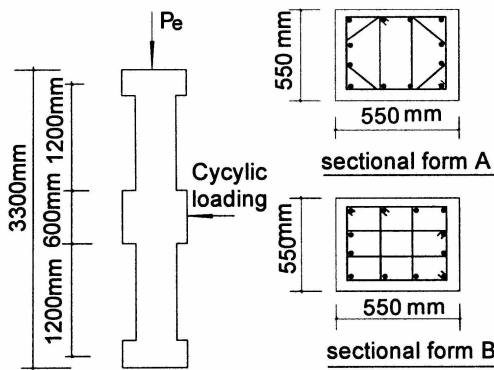


Fig. 1 Details of test specimen

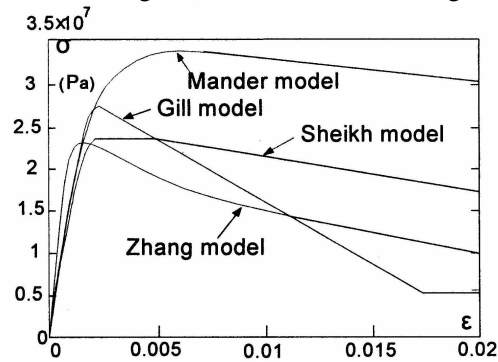


Fig. 2 Comparison of stress-strain relationships calculated from different models

CALCULATION BASED ON EACH MODEL FOR SPECIMEN 1 AT MATERIAL LEVEL

In the light of the significant difference in various confinement models at material level, only the computing results of four models for Specimen 1 are presented in this paper (Tab. 2 and Fig. 2). The results show that:

- (1) Because each model is put forward based on its own experiment, the behavior of concrete material

scatters, and experimental technique and measurement are not unified, each model is quite different at material level. For Specimen 1, the difference of f_{cc} amounts to $39.95/23.5=1.7$; the difference of ϵ_{cc} reaches to $0.0075/0.0022=3.41$.

- (2) Dispersion of descending branch is greater than that of ascending branch. The Mander model shows good ductility of the material, but the Gill model and the Zhang model show relatively poor ductility of the material.

COMPARISON OF CONFINED CONCRETE AT MEMBER LEVEL

Effect of hysteretic rules

In order to discuss to effect of different hysteretic rules, a comparison is drawn in different confined concrete models by adding hysteretic rules to them. Simulative calculations of Specimen 1 based on the Mander model after adding different hysteretic rules are only presented here. These rules are used in this paper:

- (1) Rule 1: Because the calculated stiffness of the unloading curve is larger than E_c when ϵ_U approaches to ϵ_{cc} , borrowing ideas from the Blakeley model, the unloading curve less-than ϵ_{cc} is modified to straight line and the rate of slope is E_c . The specification of ϵ_{re} and assumptions of concrete in tension are retained in the Mander model (Fig. 3).
- (2) Rule 2: Holding the specification of ϵ_{pl} and ϵ_{re} in the Mander model, the unloading curve are modified to two-fold line when ϵ_U is greater than ϵ_{cc} (Fig. 4), and
- $$\epsilon_Q = 0.5 \times (\epsilon_{pl} + \epsilon_U), \sigma_Q = 0.4 \times \sigma_U$$
- (3) Rule 3: Holding the specification of ϵ_{pl} and ϵ_{re} in the Mander model and adding Blakeley-hysteretic rules (Fig. 5). More details can be referred to Reference 8.
- (4) Rule 4: New hysteretic rules is presented in this paper: the unloading curve is modified to two-fold line when ϵ_U is greater than ϵ_{cc} (Fig. 6), and

$$\epsilon_{pl} = 0.5 \epsilon_U, \epsilon_Q = 0.75 \epsilon_U, \sigma_Q = 0.4 \sigma_U$$

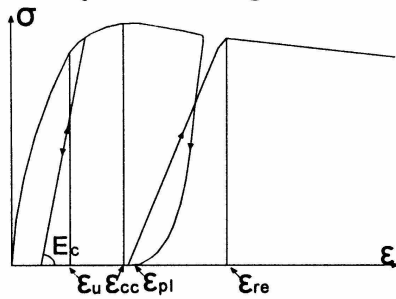


Fig. 3 Rule 1

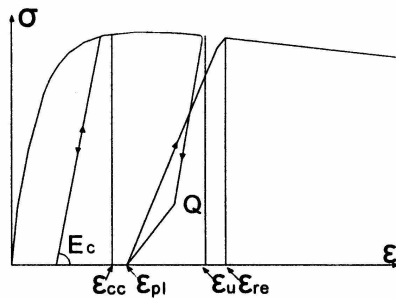


Fig. 4 Rule 2

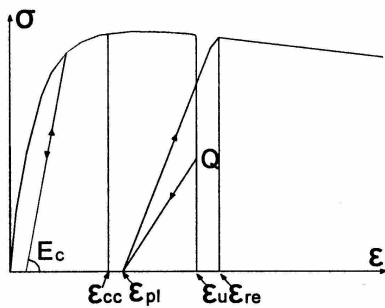


Fig. 5 Rule 3

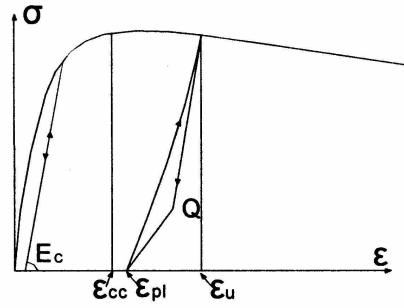


Fig. 6 Rule 4

The following can be found in Fig. 7:

- (1) When using the rule 3 to simulate, strength drops suddenly in the unloading curve of Blakeley hysteretic rules, which causes capacity and ductility of the member to reduce and the specimens have been destroyed at $u=6$.
- (2) When the deformation is small, the simulative results of three other hysteretic rules almost coincide with each other, and they are yet consistent when the deformation is relatively greater.
- (3) Hysteretic rules proposed in this paper could simulate well hysteresis characteristic of specimens, which is easy to use and code. To avoid the effect of hysteretic rules, the hysteretic rules of two-fold line presented in this paper are applied to each confined model in the following.

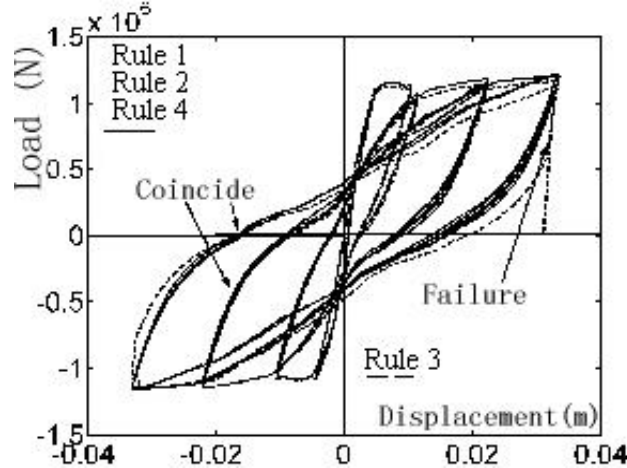


Fig. 7 The comparison among different hysteretic rules

Effect of skeleton curves

Test results of specimens at different displacement ductility u is listed in Tab. 2, which is corresponding to computing results of loading at $u=2, 4$ and 6 . Fig.8, 10, 12, 14, 15 and 16 show simulative results of different models on four specimens. For the sake of figure clarity and because of no failure of specimen 1 and 2 in simulation, only one hysteresis loop is shown in Fig.8 and 10 at each ductility ratio respectively. Fig.9, 11, 13 and 17 are experimental curves of four specimens.

Tab. 2 The force of each specimen calculated by each model according to $u=2,4$ and 6 (*'= near failure)

Specimen	Displacement (mm)	Test result (KN)	Mander Model (KN)	Zhang Model (KN)	Sheikh Model (KN)	Gill Model (KN)
1-1	10.5	1267	1134	1061	1060	1086
1-2	22.5	1311	1185	1038	1050	1061
1-3	33.72	1317	1204	980*	1022	943
2-1	8.477	1402	1434	1425	1346	1461
2-2	17.02	1410	1360	1334	1348	1380
2-3	25.65	1417	1398	1335	1374	1388
3-1	6.98	1205	1182	1071	1092	1169
3-2	14.0	1175	1218	998*	1046	1067
3-3	20.93	1166	1208	938*	1002	559
4-1	5	1225	1219	1053	1058	1248
4-2	0	1387	1301	999	991	1187
4-3	15.5	1416	1341	1135*	965	failure

It can be observed that:

- (1) The difference of simulative results at member level for each model are less than that at material level, and the max is $1341/965=1.39$.

- (2) When ductility is small ($\mu=2$), the difference of computing results of capacity of each model is small; with increasing of ductility, the difference becomes large gradually.
- (3) When the ratio of axial compress force to strength is small (Specimen 1 and 2), the variance of calculative results among these models is small; with increasing of the ratio, the variance grows.
- (4) Simulative results of the Mander model and the Sheikh model are comparatively satisfactory, and those of the Zhang model and the Gill model have been destroyed at high ductility. The Mander model is the best in simulative results.

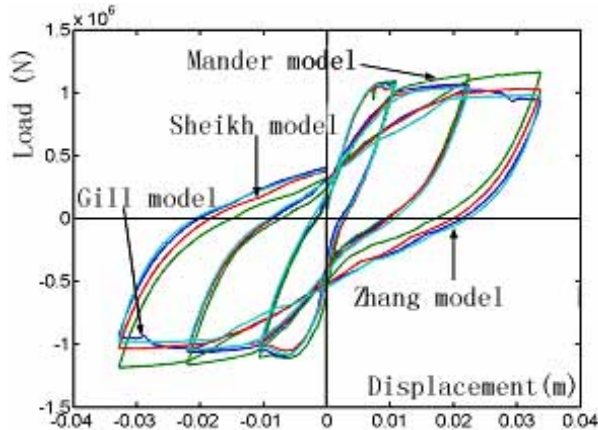


Fig. 8 The simulated comparison of Specimen 1

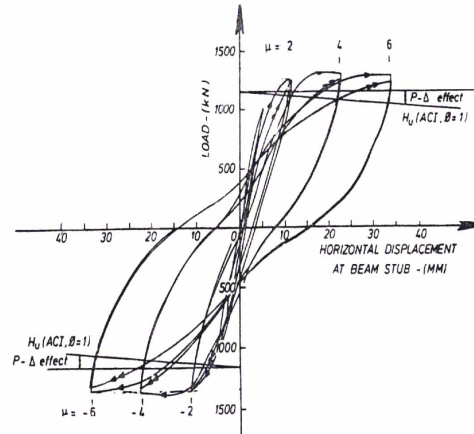


Fig. 9 Test result of Specimen 1

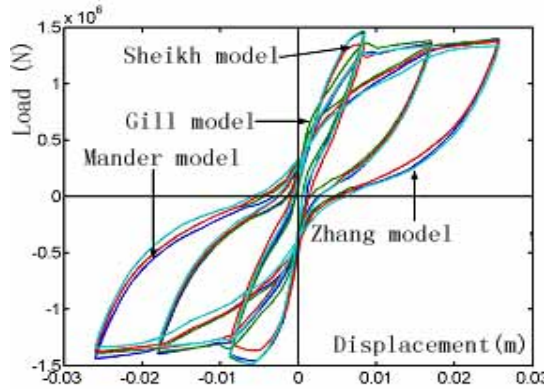


Fig. 10 The simulated comparison of Specimen 2

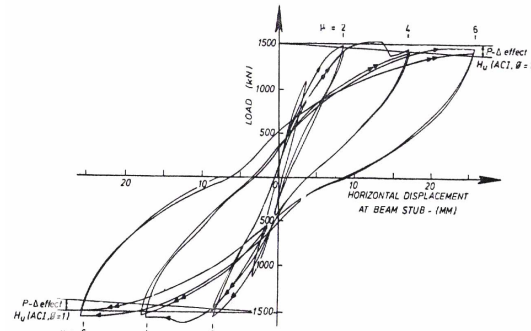


Fig. 11 Test result of Specimen 2

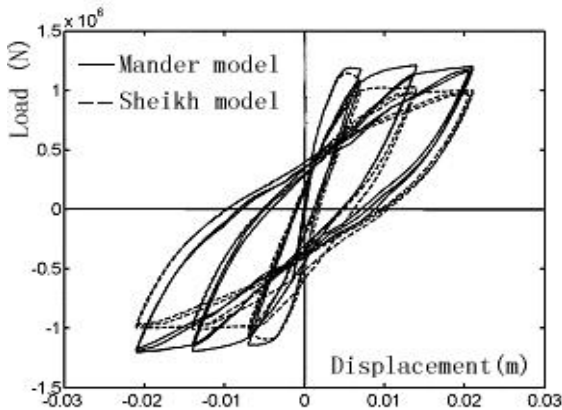


Fig. 12 The simulated comparison of Specimen 3 between the Mander model and the Sheikh model

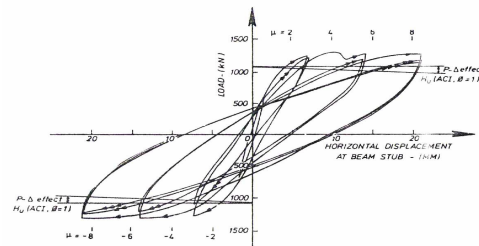


Fig. 13 Test result of Specimen 3

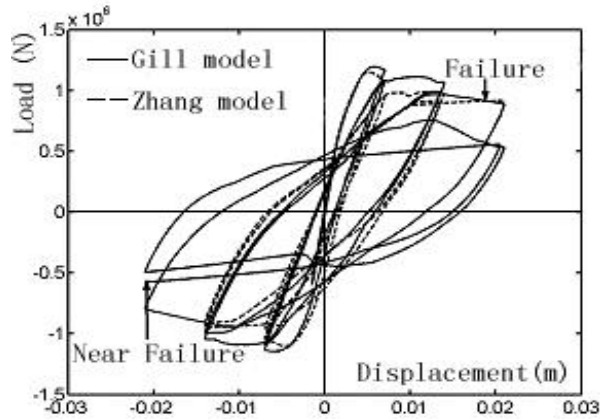


Fig. 14 The simulated comparison of Specimen 3 between the Zhang model and the Gill model

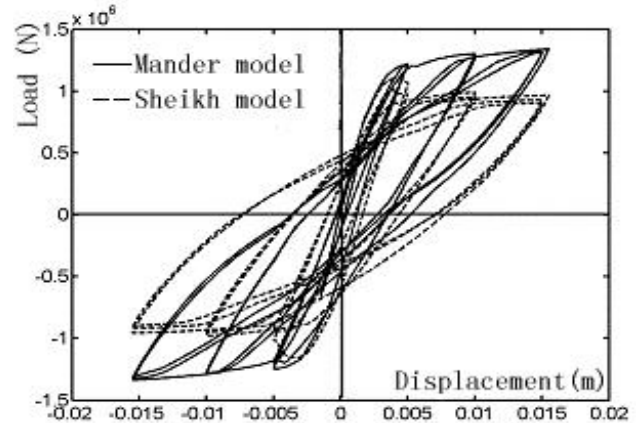


Fig. 15 The simulated comparison of Specimen 3 between the Mander model and the Sheikh model

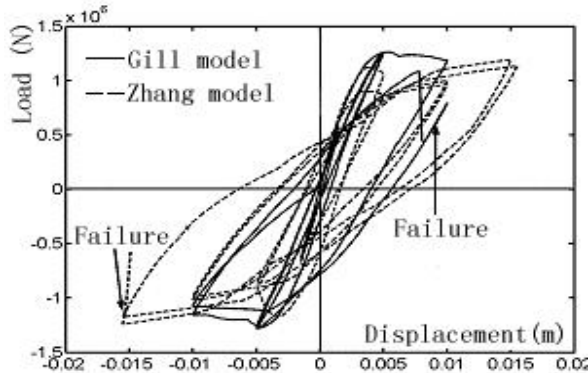


Fig. 16 The simulated comparison of Specimen 4 between the Zhang model and the Gill model

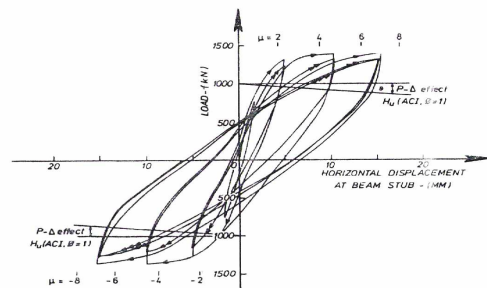


Fig. 17 Test result of Specimen 4

CONCLUSION

1. A significant difference exists in stress-strain relationships of different confined concrete models. In member analysis, although the difference has been greatly reduced, but still is remarkable. Thus, the confined concrete model should be carefully selected in structural analysis.
2. Skeleton curves and hysteretic rules play an important role in numerical simulation at structural member.
3. The primary factor affecting simulative accuracy of confined concrete at member level is ductility of descending branch in the material model, which is just the maximal dispute among the current models. The main factors affecting the mechanical behavior of confined concrete should be further investigated.
4. The results in this paper show that the Mander model obtained the better agreement with the test results.

REFERENCES

1. Mander J. B, Priestley M. J. N and Park. R. "Theoretical stress-strain model for confined concrete". J Strut Div ASCE, 1988; 114(8): 1804-1826.
2. Park R. Priestley. M. J. and Gill W. D. "Ductility of square-confined concrete columns". J Struct Div ASCE, 1982; 108(4): 929-950.

3. Park.R. Kent D.C. and Sampson R.A. "Reinforced concrete members with cyclic loading". J Stuct Div ASCE,1972; 98(7): 1341-1359.
4. Sheikh S.A. "A comparative study of confinement models". ACI Struct J,1982; 79(4):296-306.
5. Sheikh S. A and Uzumeri S. M. "Analytical model for concrete confinement in tied columns". J Struct Div ASCE,1982;2703-2722.
6. Thompson K. J and Park R. "Moment-curvature behavior of cyclically loading structural concrete members". Proceedings of the Institution of Civil Engineers (London). Part 1 - Design & Construction. 1980;69(2): p317-341.
7. Yankelevsky D. Z, Reinhardt H. W. "Model for cyclic compressive behavior of concrete". J Struct Engng ASCE,1987;113(2);228-240.
8. Zhang Xiuqin, Guo Zhenhai, Wang Chuanzhi. "Stress-stain curvilinear equation of confined concrete under cyclic loading". J Building Structure,1982;9:16-20.
9. Spacone E., Filippou F.C., and Taucer F.F. "Fiber beam-column model for non-linear analysis of R/C frames: Part I. Formulation". Earthquake Engineering and Structural Dynamics, 1996; 25: 711-725.
10. Filippou F.C., Popov E.P., and Bertero V.V. "Modeling of reinforced concrete joints under cyclic excitations". J Struct Engng ASCE;109(11):2666-2684.

NOTATION

The following symbols are used in this paper

f_c = compressive strength of confined concrete;

f_{yh} = tie yield strength;

ϵ_U = the strain corresponding to the unloading point;

ϵ_{cc} = the strain corresponding to the maximum concrete stress;

ϵ_{pi} = the strain corresponding to the unloading point whose stress is zero;

ϵ_{re} = the strain corresponding to the intersection between reloading curve and skeleton curve;

ϵ_Q = the strain corresponding to Point 'Q';

E_c = the tangent modulus of elasticity of the concrete;

σ_U = the stress corresponding to the unloading point;

σ_Q = the stress corresponding to Point 'Q'.